

Chemoenzymatic Route to Renewable Thermosets Based on a Suberin Monomer

Arne Rüdiger^{1,2}, Peter Hendil-Forsell³, Cecilia Hedfors³, Mats Martinelle³, Stacy Trey^{4,5,*}, Mats Johansson^{1,4}

¹Department of Fibre and Polymer Technology, KTH Royal Institute of Technology, Stockholm, Sweden

²Department of Coating Materials and Polymers at the University of Paderborn, Paderborn, Germany

³Department of Biochemistry, KTH Royal Institute of Technology, Stockholm, Sweden

⁴Wallenberg Wood Science Centre (WWSC), KTH Royal Institute of Technology, Stockholm, Sweden

⁵SP Träteknik, SP Technical Research Institute of Sweden, Stockholm, Sweden

Received November 1, 2012; Accepted January 10, 2013, Published online February 1, 2013

ABSTRACT: The present study describes the use of an epoxy functional fatty acid, 9,10-epoxy-18-hydroxyoctadecanoic acid (EFA), extracted from birch (*Betula pendula*) outer bark to produce thermosets. The purified epoxy fatty acid was polymerized by enzyme-catalyzed polycondensation utilizing *Candida antarctica* lipase B (CalB) to form oligomers with targeted degrees of polymerization (DP) of 3, 6, and 9 and obtained DPs of 2.3, 5.9 and 7.3, respectively. It was determined that it is possible to first enzymatically polymerize and aliphatically endcap the epoxy functional fatty acid resulting in controlled oligomer lengths while also maintaining the epoxy functionality for further reaction by main-chain homo-epoxy cationic photopolymerization. The enzymatic polymerized oligomers were characterized in terms of conversion of the residual epoxy groups (FT-IR), the thermal properties (DSC, TGA) and the purity by MALDI-TOF and ¹H-NMR. The amorphous thermoset films with varying degrees of crosslinking resulting from the cationically photopolymerized oligomers, were characterized in terms of their thermal properties and residual epoxy content (FT-IR ATR). The crosslinked polyesters formed insoluble, amorphous, and transparent films. This work demonstrates that thermoset films with designed properties can be effectively made with the use of forest products to reduce the petroleum-based plastics market.

KEYWORDS: Suberin, natural epoxidized oils, enzyme-catalyzed polymerization, cationic photopolymerization

1 INTRODUCTION

Large resources and efforts have been put forth in recent history in a concerted drive to replace a large amount of petroleum-based plastics with building blocks that are derived from natural and renewable resources. This is evident from the range of natural products-based plastics that are now entering the market, and the number of government recommendations and reports being published, which target potential renewable monomers as plastic building blocks [1, 2]. What is more, examples of polymers with designed and tailored properties derived from plant oils are now abundant in the literature [3–12]. The waste streams from the facilities of the pulp and paper industry present a rich source of renewable chemicals [13]. The birch tree (*Betula pendula*) is used

in the paper and pulp industry as a raw material, meaning that there is a large amount of residual outer birch bark that is currently burned for the extraction of energy. The birch tree is an important raw material for pulp and paper production in the Nordic countries, with a pulp production of 400,000 tons per year that generates about 28,000 tons per year of outer birch bark [14, 15]. As an alternative for use in biofuel, the possibility of extracting renewable monomers from outer birch bark and producing plastics is beginning to be investigated in order to raise the value of this commodity. The extractives include a broad range of functional fatty acids, or approximately 27 wt% of the dried outer birch bark, with functionalities including mid-chain epoxy and hydroxyl groups, along with dicarboxylic and hydroxyl end-chain reactive groups [16–18]. The second most abundant fatty acid in birch bark, 9,10-epoxy-18-hydroxyoctadecanoic acid (EFA), amounting to 9.9 wt% of dried outer birch bark, has previously been used for polyester synthesis, by first extracting with a mild alkaline hydrolysis to leave the

*Corresponding author: stacy.trey@sp.se

DOI: 10.7569/JRM.2012.634109

mid-chain epoxide group intact [19]. These reactive monomers from suberin have been further reacted to form polyesters by various methods [20–24].

Enzyme-catalyzed polymerizations represent an attractive method to obtain desired polyester polymers that would otherwise be impossible or extremely laborious under conventional synthesis methods. This has become a well-developed field due to the positive aspects and endless possibilities regarding this type of polymerization [25–29]. Enzymes are highly selective and include chemo-, enantio- and regioselectivity, and often catalyze only one substrate or one specific reaction. Although this concept is found to have exceptions, the so-called “enzyme promiscuity” that scientists are finding can be a for further optimization for use in designing new materials [30]. *In vitro* enzyme-catalyzed polymerizations are typically less toxic than conventional metal catalysts and operate under mild thermal conditions, reducing the required reaction energy. This in combination with enzyme regioselectivity, enables the preservation of functional groups [31]. In nature, *Candida antarctica* lipase B (CalB) catalyzes the hydrolysis of fatty acid glycerol esters. However, by working in nonaqueous media and by constantly removing condensation by-products, CalB catalyzes polycondensations. It is also capable of catalyzing reactions at high temperatures (stable at temperatures of 90–100°C) and in organic solvents [17, 32]. Previous studies done by Olsson *et al.* report successful enzyme-catalyzed polymerizations of 9,10-epoxy-18-hydroxyoctadecanoic acid to high molecular weights of around 40 kDa with the use of CalB [13].

Cationic photopolymerization is one of the fastest growing areas in the UV-cure industry, with large application in printing [33]. Advantages include comparatively low cure shrinkage, energy efficient cure, solvent-free synthesis, and mild cure temperatures. Epoxy-based polymers are best known for their adhesion and chemical resistance [34, 35]. In addition, diaryliodonium salt photoinitiators have provided a further advantage as they are benzene free and thermally stable at room temperature, while providing solubility with a broad range of systems [36–38]. Although epoxide groups located in the main chain are less reactive than pendant epoxide groups, they can still be incorporated into thermosets in an effective way [39, 40].

The purpose of this work is to demonstrate the possibility for using the epoxy functional fatty acid extractive derived from outer birch bark as a renewable resource in designing controlled and functional oligomers. Another purpose is to demonstrate the versatility of making oligomers, while ensuring that the epoxy groups remain intact on the main chain,

enabling further reaction at a later time. This is not easily done by conventional polymerization methods. At the same time, the oligomers are endcapped, in this case chosen to be nonfunctional, in order to produce main-chain epoxy functional oligomers of controlled length. The functional oligomers are then further reacted by cationic photopolymerization to produce thermoset films with properties being a result of the oligomer size.

2 EXPERIMENTAL

2.1 Materials

All chemicals were purchased from Sigma-Aldrich unless otherwise noted. Novozyme 435 (Immobilized lipase B from *Candida antarctica*) was dried under vacuum (5 mbar at 21°C for 48 h). Hexyl octanoate and EFA reactant mixtures were dried over activated molecular sieves. The photoinitiator phenyl-p-octyloxyphenyl-iodonium hexafluoroantimonate (Uvacure 1600) was obtained from Cytec. Outer birch bark of *Betula pendula* was gathered from the forest in the local Stockholm region. The bark was dried at room temperature for 72 h then finely ground using a ZM 200 (Retsch) grinder.

2.2 Methods

2.2.1 Removal of Extractives

The isolation of the product was performed according to the literature [13, 41]. Outer birch bark extractives were removed by Soxhlet extraction using n-heptane as the solvent so that they would not interfere with the subsequent alkaline hydrolysis. Soxhlet extraction was conducted with 170 g of outer birch bark that was finely ground and placed in a cotton container, and 2.5 L n-heptane that was refluxed for 8 h at a time. The n-heptane was left to cool overnight, and starting the next morning the precipitate in the room temperature n-heptane was vacuum filtered daily. The extraction was repeated daily, for 5 days, until a negligible amount of precipitates occurred. Filtration of the precipitates yielded a white powder (47 g, 28 wt% of outer birch bark) with a light-yellow glimmer that was characterized by NMR to be betulin and was not used in this study. The remaining outer birch bark was air dried for further processing.

2.3 Hydrolysis Process

The extracted birch bark was then subjected to alkaline hydrolysis to depolymerize the 3D structure of suberin; 100 g was placed in a 2 L round-bottom flask

containing a magnetic stirrer. Isopropanol (1150 mL, 96 vol% of the solution) and an aqueous NaOH solution (50 mL, 11 M) were added to the flask. The solution was refluxed with continuous stirring for 1 h. After leaving the solution to cool to approximately 50–60°C, the solute was separated from the bark residues by warm vacuum filtration. The bark residues were then refluxed again in 500 mL of isopropanol for 20 min. The bark was separated from the solution as previously described. Both isopropanol solutions were combined and condensed at 40°C using a rotary evaporator to reduce the volume of the solution by about 50% (900 mL isopropanol was evaporated). The precipitate was mixed with 650 mL water and stirred for 2 h at room temperature. The precipitate was then separated from the solution of isopropanol/water by centrifuge, resulting in a clay-like precipitate.

This precipitate (with the solute fraction further processed to result in Fraction 2) centrifuged from the 650 mL of water and 250 mL of isopropanol, was mixed with 200 mL water and acidified to pH 4.7 using dilute hydrochloric acid (5%). The precipitate was separated by centrifuge and freeze-dried. This fraction (Fraction 1) was characterized as 22-hydroxydocosanoic acid and was not used in this study (yield: 13.4 g, 9.7 wt% of dried outer birch bark).

The solute obtained (with the precipitate of Fraction 1 processed as described above) was acidified to pH 5.0 using HCl (5%), resulting in precipitates. These precipitates were separated from the solution by centrifuging and freeze-drying. This fraction (Fraction 2) was identified as 9,10-epoxy-18-hydroxyoctadecanoic acid by ¹H NMR (10.3 g, 7.4 wt% of dried outer birch bark) and was light yellow in color. This yield is similar to reported values [17]. Fraction 2 was found to contain a small degree of impurities as determined by thin-layer chromatography with EFA having an R_f value of 0.28 and the impurity an R_f value of 0.42 in 60/40 (vol%) ethyl acetate/n-heptane.

2.3.1 Purification via Column Chromatography

Fraction 2 was purified via column chromatography. Column chromatographs were performed with 2 g of EFA using a conventional column having a diameter of 2.5 cm (filled with 20 cm silica). Due to the moderate solubility of the samples in the starting eluent mixture, the samples were dissolved in chloroform and mixed with 20 g of silica, the solvent was evaporated and the solid mixture was added to the top of the column. A polarity gradient was used as eluent to provide better separation. The starting eluent was a mixture of ethyl acetate and n-heptane at a ratio of 50/50 (vol%). The polarity was increased up to pure ethyl acetate in increments of ten (60/40 (vol%), 70/30 (vol%), etc.). To provide good separation 100 mL of each mixture was used with the exception of pure ethyl acetate (250 mL).

2.3.2 Enzyme-Catalyzed Synthesis of EFA Oligoesters

The immobilized *Candida antarctica* lipase B catalyst Novozym 435, was utilized as the catalyst for the polyesterification reactions. EFA was combined with the enzyme and hexyl octanoate as the endcapper with targeted degrees of polymerization (DP) of 3, 6, and 9 (Figure 1).

Capped reaction vials were charged with EFA (DP 3: 100.4 mg, 0.33 mmol; DP 6: 126.4 mg, 0.40 mmol; DP 9: 135.4 mg, 0.43 mmol) and hexyl octanoate (DP 3: 24.2 mg, 0.11 mmol; DP 6: 15.3 mg, 0.07 mmol; DP 9: 10.9 mg, 0.05 mmol). Molecular sieves (50 mg) and toluene (1 mL) were added to each mixture. The addition of Novozym 435 (DP 3, 6, and 9: 25 mg) initiated the reactions, which were carried out for 72 h at 60°C using a HLC PROGR (DITABIS) thermomixer. The reaction vials were constantly shaken during reaction time. The reactions were stopped by filtering off the enzyme.

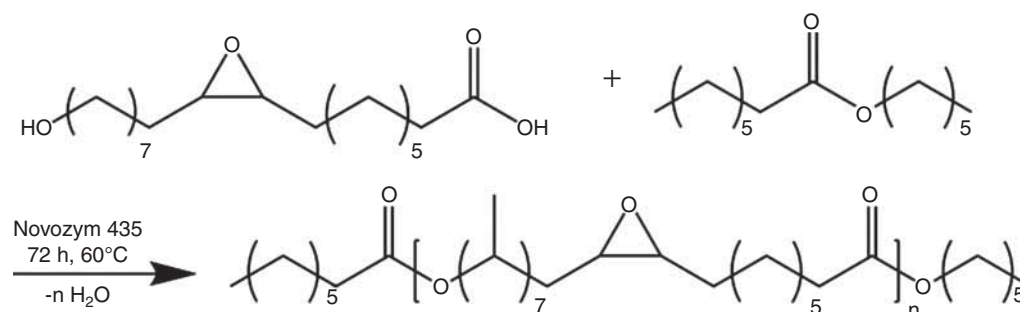
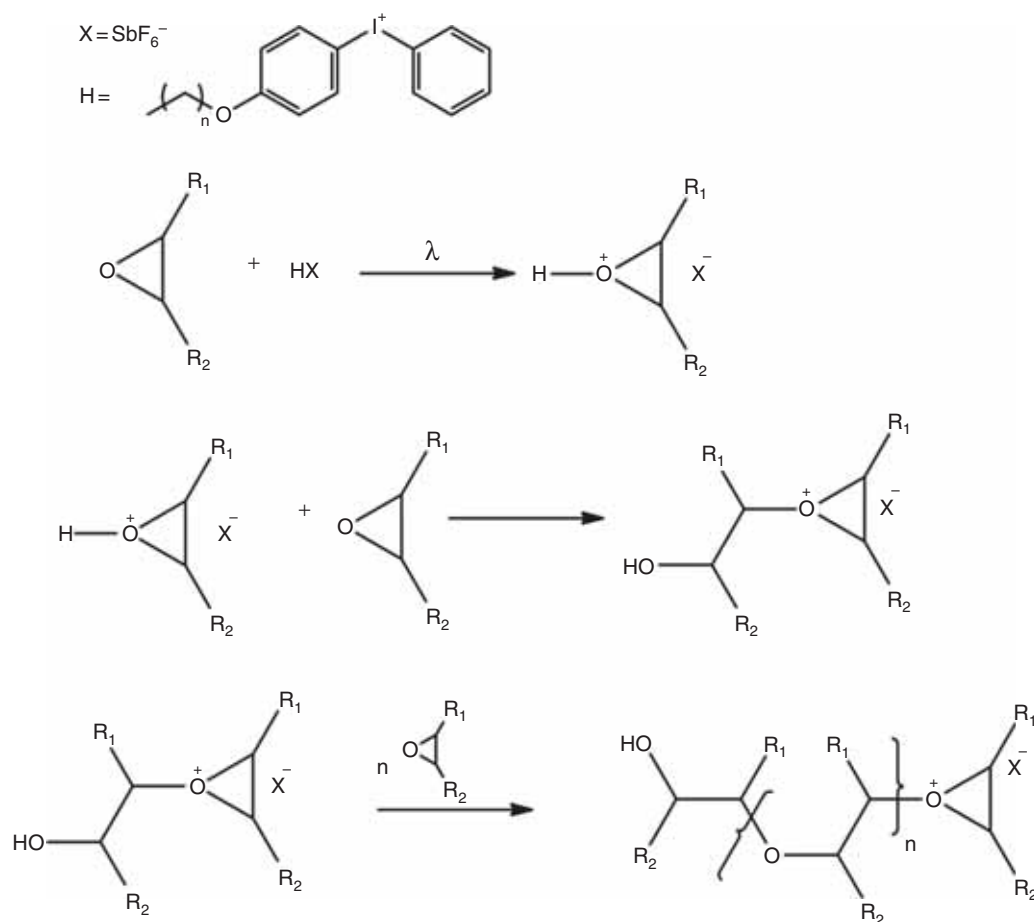


Figure 1 Enzyme-catalyzed polycondensation of endcapped oligoesters.

Table 1 Amounts and yields of enzyme-catalyzed polymerizations.

DP	EFA, mg (mmol)	hexyl octanoate, mg (mmol)	Novozym 435 (mg)	Yield (%)
3	100.4 (0.33)	24.2 (0.11)	24.9	70
6	126.4 (0.40)	15.3 (0.07)	25.5	69
9	135.4 (0.43)	10.9 (0.05)	25.2	85

**Figure 2** Cationic photopolymerization of main-chain epoxy functional oligomers [36].

Subsequently toluene was evaporated under reduced pressure and the residue was dried in a vacuum oven at 50°C to give wax-like products (DP 3: 87 mg, 70%; DP 6: 98 mg, 69%; DP 9: 125 mg, 85%). Table 1 summarizes the used amounts of compounds and yields.

2.3.3 Cationic Photopolymerization of Oligomers

The synthesized polyesters were crosslinked without any further purification steps using Uvacure 1600 as the cationic initiator (Figure 2.). Vials were charged with each DP of the synthesized polyesters (25 mg

of DP 3, DP 6 and DP 9, respectively), Uvacure 1600 (1 mg) and chloroform (100 mg). The homogenous mixtures were applied to a Teflon mold and heated in an oven at 70°C for 5 min to evaporate the solvent and heat the polymers to above their T_m in order to react in the liquid state. Afterwards, the prepolymeric mixtures were covered with a quartz microscope slide. Films were cured under a UV Fusion Conveyor MC6R. The samples were passed under the light 5 times with a dose of 150 mJ cm⁻² per passage, to give an overall dose of 750 mJ cm⁻² and then left at room temperature to cool down. Transparent films were obtained, which were insoluble in chloroform.

Table 2 Naming scheme.

Abbreviation used in text	Explanation
EFA	9,10-epoxy-18-hydroxyoctadecanoic acid (monomer)
EFA-DP3	oligoester of DP3
film-DP3	thermoset after photopolymerization of EFA-DP3
EFA-DP6	oligoester of DP6
film-DP6	thermoset after photopolymerization of EFA-DP6
EFA-DP9	oligoester of DP9
film-DP9	thermoset after photopolymerization of EFA-DP9

The names of the samples are summarized according to Table 2.

3 ANALYTICAL METHODS

3.1 ¹H-NMR

¹H- and ¹³C-NMR analyses were performed on a Bruker Avance 400 at a resonance frequency of 400 MHz using deuterated chloroform as solvent. NMR spectra were used for characterization of the monomer and oligoesters.

NMR data of 9,10-epoxy-18-hydroxyoctadecanoic acid obtained from fraction 2:

¹H-NMR (CDCl₃), δ (ppm): 1.3-1.7 (26H, m, -CH₂-), 2.4 (2H, t, J=7.4Hz, -COCH₂-), 2.9 (2H, s, -CH-epoxide), 3.7 (2H, t, J=6.6Hz, -CH₂OH).

¹³C-NMR (CDCl₃), δ (ppm): 24.65-33.83 (14C, -CH₂-), 57.27-57.30 (2C, -CH- epoxide, C-9 and C-10), 63.04 (1C, -CH₂OH, C-18), 178.39 (1C, C=O, C-1).

3.2 Matrix-Assisted Laser Desorption/Ionization – Time of Flight Mass Spectroscopy (MALDI-TOF-MS)

Measurements were conducted on a Bruker UltraFlex MALDI-TOF MS with a SCOUT-MTP Ion Source (Bruker Daltonics) equipped with a nitrogen laser (337 nm). Measurements were used to analyze the synthesized polyesters in regards to the repeating unit and the distribution of polymer lengths. As for the samples, 1 mg of each DP was dissolved in 1 mL chloroform. The matrix solution utilized was 1,8,9-antracenetriol (10 mg/mL) dissolved in THF, and the salt solution used was trifluoro acetic acid (1 mg/mL) in THF. The samples were prepared by mixing 5 μL of each with 20 μL of matrix solution and 5 μL of salt solution. Subsequently 0.5 μL were added to the MALDI target plate and left at room temperature to evaporate the solvent.

3.3 Size Exclusion Chromatography (SEC)

SEC was conducted at 35°C using THF (10 mL/min) as the mobile phase using a Viscotek TDA model 301 equipped with two T5000 columns containing porous styrene divinylbenzene copolymer, a VE 2500 GPC autosampler, a VE 1121 GPC solvent pump and a VE 5710 GPC degasser. A conventional calibration method was created using narrow linear poly(methyl methacrylate) standards (MW ranging from 805–400,000 Da). Measurements were performed with the oligoesters to analyze molecular weight distributions. For the measurements a sample of each oligoester dissolved in THF was prepared (DP 3: 2.6 mg/mL; DP 6: 2.9 mg/mL; DP 9: 2.9 mg/mL).

3.4 Differential Scanning Calorimetry (DSC)

Thermal properties of the monomer, polyesters and crosslinked polyesters were analyzed by DSC measurements. Experiments were performed on a DSC 820 equipped with a sample robot and a cryocooler (Mettler-Toledo). The DSC runs were carried out in closed sample pans sealed in air using the following temperature program: heating from 25°C to 100°C (50 °C/min), cooling from 100°C to -30°C (10°C/min) and then heating up to 100°C (10°C/min). Isothermal segments of 5 min were performed at the close of each dynamic segment.

3.5 Thermal Gravimetric Analysis (TGA)

TGA measurements were performed to determine degradation temperatures and weight losses due to volatilization and degradation of the monomer, polyesters and crosslinked polyesters. The experiments were conducted on a TGA/SDTA 851^e (Mettler-Toledo) with a sample robot. The TGA runs were carried out in nitrogen atmosphere (20 mL/min) heating the sample from 25°C up to 700°C (10°C/min).

3.6 FT-IR Spectroscopy

FT-IR spectra were obtained for EFA, the oligoesters, and the crosslinked films to determine the availability of the epoxy groups. Measurements were performed on a Perkin-Elmer Spectrum 2000 FT-IR equipped with a heat controlled single reflection attenuated total reflection (ATR) accessory (Golden Gate heat controlled). Each spectrum was based on 32 scans in reflection mode.

4 RESULTS AND DISCUSSION

4.1 The Extraction Process

Outer birch bark extractives were removed by Soxhlet extraction, and the remaining bark was hydrolyzed and EFA was extracted according to Kratusky *et al.* [17]. After removal of Fraction 1, it was of utmost importance to keep the pH above 5 in order to preserve the epoxy ring in the main chain of the fatty acid. When the pH dropped below 5, the epoxy ring was opened to form two hydroxyl groups on adjacent carbons on the main chain. In this case, the pH was kept above 5 to receive Fraction 2, and this was further purified by flash chromatography. The yield of EFA was slightly lower than the reported values of Kratusky *et al.*, and this could be a combination of many factors such as source, type of birch bark, and equipment used for the extraction process. The optimization of this process was outside the scope of this work.

4.1.1 Purification of the Epoxy Fatty Acid

After column chromatography a much smaller yield was received than expected, with 64.5% weight loss of 9,10-epoxy-18-hydroxyoctadecanoic acid obtained and a yield of 35.5 wt%. This is suspected to be due to the fact that acid functionalities have been documented to adhere strongly to the column, and a common solution is the addition of an acid to the eluent. However, this would negatively result in the ring-opening of the epoxy group on the monomer and so could not be tried in this case. Therefore, there is a need for further optimization of separation by chromatography, with the possible use of different types of column packing materials or optimization of purification by crystallization.

The original yellow color of the powder was observed to be left on the column, which was assumed to be aromatics, based on NMR analysis in which the peak at 2.1 ppm attributed to phenol groups was significantly decreased, and the final product was white. The following figure shows the ^1H NMR spectrum of the isolated and purified epoxy fatty acid from Fraction 2 (Figure 3).

4.1.2 Enzymatic Polymerization of the Epoxy Fatty Acid

Purified EFA obtained from Fraction 2 was used for enzyme-catalyzed polymerizations with degrees of polymerization of DP 3, DP 6 and DP 9 utilizing CalB as the enzyme catalyst and hexyl octanoate as the endcapper. The endcapper ensured control of the length of the

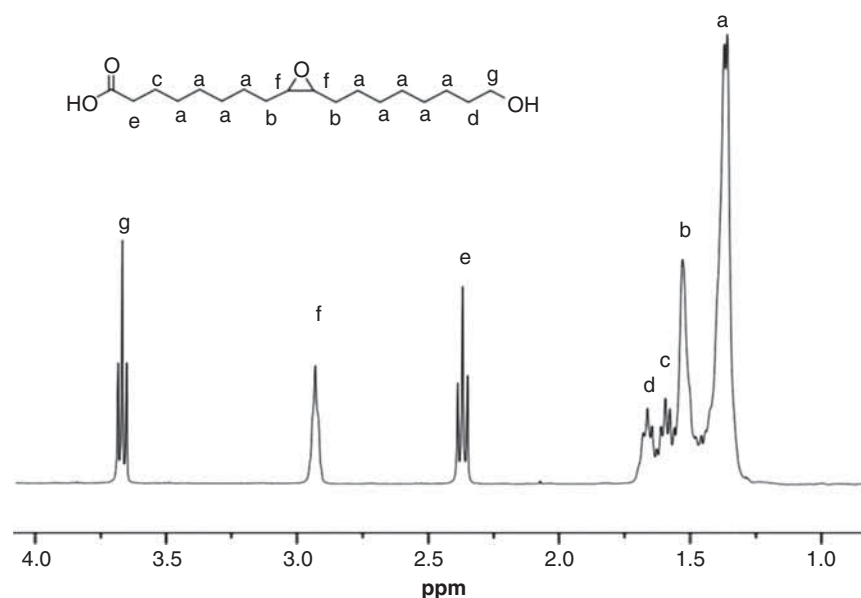


Figure 3 ^1H -NMR spectrum Fraction 2 after column chromatography.

oligomers along with the stoichiometry. This method also allowed for end groups to undergo polycondensation while the epoxy group was left unmodified on the main chain as a result of the selectivity of CalB along with the mild temperatures. The aim of this was to link together the monofunctional epoxy EFA in chains of 3, 6, and 9, leaving the epoxy group intact, to provide oligomers with a corresponding average number of epoxy functionalities on the main chain of 3, 6, and 9. No problems with solubility were observed as the oligomers were formed. This was expected as the reaction was performed in toluene, as previous studies have shown this to be a favorable solvent for the reaction.

4.1.3 Characterization of Oligoesters

The synthesized polyesters (hereafter named as EFA-DPX, where the value of X is dependent on the DP) were analyzed by NMR, SEC and MALDI-TOF measurements to determine their molecular structures and molecular weight distributions. All three analytical methods confirm successful polymerizations resulting in polyesters with varying DPs. The yields of 70, 69 and 85% for DP 3, 6, and 9 are lower than expected, and this was attributed to losses of material during processing steps. No optimization with respect to product recovery

was performed. The DPs of the synthesized polyesters were calculated from acquired NMR spectra. Figure 3 shows the NMR spectrum belonging to EFA-DP6, with the majority of the product represented by the first structure 1, with structures 2 and 3 illustrating minor fractions. The α -protons to the carbonyl groups of the oligomers that have not been capped (structure 3, Figure 4) are observed by the shoulder of peak e (Figure 4). However the exact hydroxyl content is also difficult to quantify because it is combined with a small impurity, but is still observed to a small extent, by the proton of the methylene group neighboring the hydroxyl group (peak g). The NMR spectrum further confirms that the epoxy groups at 2.9 ppm are still intact.

The synthesized DP was calculated by normalizing all integrals to the methyl groups i of the endcapper at 0.9 ppm and multiplying by 2 (to give the value of 6 protons), assuming 100% endcapped oligomers. This is then divided into the integral of h (4.1 ppm), indicating the 2 protons by the ester, multiplied by 6 and subtracting 1 to account for the proton of the alcohol endcapper (Eq. 1).

$$DP(\text{exp.}) = \left(\frac{h \times 6}{i \times 2} \right) - 1 \quad (1)$$

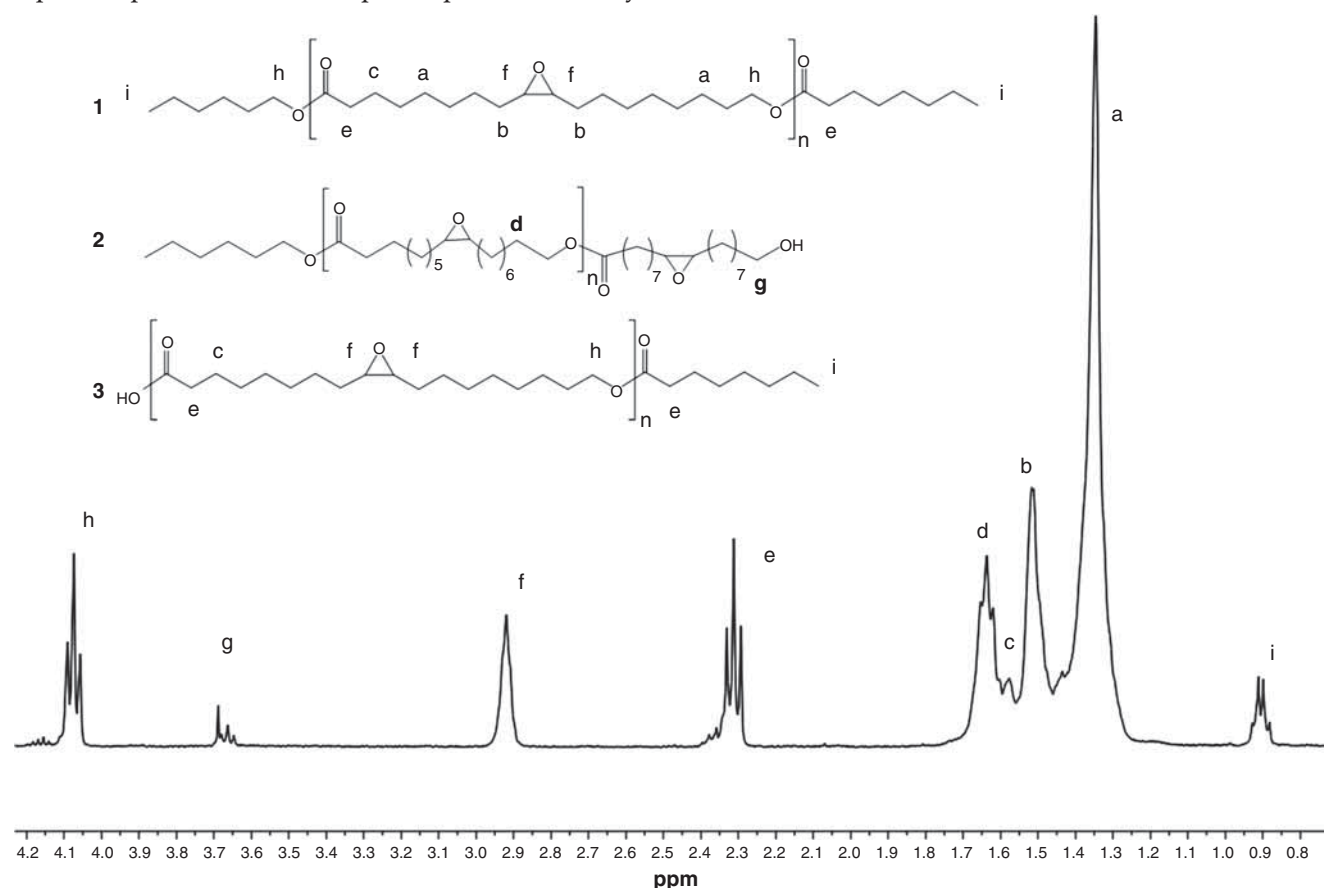


Figure 4. ^1H -NMR spectrum and structural formula of EFA-DP6.

Additional ^1H NMR spectra corresponding to EFA-DP3 and EFA-DP9 are represented in the supplementary information. The resulting DPs determined by NMR measurements are DP 2.3 (3), DP 5.9 (6) and DP 7.3 (9), respectively (theoretical values in brackets). Furthermore, the calculated integrals of the acquired NMR spectra show that the obtained polyesters are not completely endcapped. The SEC measurements further confirm successful enzyme-catalyzed oligomerization of EFA to different DPs (Table 3).

Differences between the DP data as determined by SEC and NMR can be attributed to the fact that the molecular weights obtained from the SEC measurements are in regards to poly(methyl methacrylate) standards and thus could have a systematic error.

MALDI-TOF MS spectra were acquired for the synthesized polyesters larger than 500 Da since the range below was dominated by peaks from the matrix.

Figure 4 shows the spectrum of EFA-DP9, with Table 4 describing the marked peaks.

In addition to the NMR and SEC results, the MALDI-TOF MS measurements confirm a successful enzyme-catalyzed polymerization of EFA resulting in different DPs. The repetitive pattern verifies the molecular weight of the repeating unit of 296 Da (see the difference of molecular weights between peak d and h in Figure 5).

The MALDI-TOF MS results also confirm that some of the synthesized oligomers are not completely endcapped, since the spectra show both cyclic structures and one type of partially endcapped oligomer (Structure 2, in Figure 3). It should be noted that this is not a quantitative analysis method, and thus the sizes of the peaks do not indicate quantities, only how effectively different fragments ionize.

In summary, the performed NMR, SEC and MALDI-TOF MS measurements all indicate that the

Table 3 Molecular weights of the synthesized oligoesters.

Polyester	DP ^a	M _n ^a in g/mol	M _n ^b in g/mol	PDI ^b
EFA-DP3	2.3 (3)	860 (1118)	1647	1.8
EFA-DP6	5.9 (6)	1970 (2007)	2159	1.9
EFA-DP9	7.3 (9)	2350 (2896)	2305	2.1

^a Determined with NMR (theoretical value within brackets).

^b Determined with SEC.

Table 4 Description of marked MALDI-TOF MS peaks; a molecular weight of repeating unit is 296.5 Da.

Peak abbrev.	a	b	c	d	e	f	g	h	i
m/z	548	616	718	844	1140	1436	1733	2030	2920
No. repeating units	1	2	2	2	3	4	5	6	9
Structure	Full (str. 1, fig. 3)	(cyclic)	Partial (str. 2, fig.3)	full	full	full	full	full	full

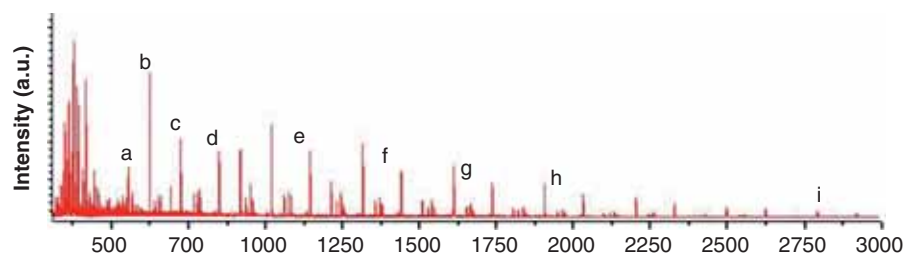


Figure 5 MALDI-TOF MS spectrum of EFA-DP9.

experimental lengths of the oligoesters are close to the targeted DPs. It is possible that the synthesis can be further optimized in an attempt to gain greater control and more accurate lengths in terms of the targeted DP by determining the ideal length of the reaction. Further, it is proposed that water is building up with time and thus the reaction is not able to proceed to completion.

4.1.4 Cationic Photopolymerization

The synthesized polyesters with varying DPs were crosslinked using Uvacure 1600 as the cationic initiator and UV radiation as the inducing energy source. The crosslinking process resulted in transparent films.

The obtained films were insoluble in chloroform, which indicated a successful crosslinking. Moreover, because of high conversion of the epoxy groups with a chain functionality of 3–9, the crosslinking reaction is further confirmed (Figure 6). The spectra indicate

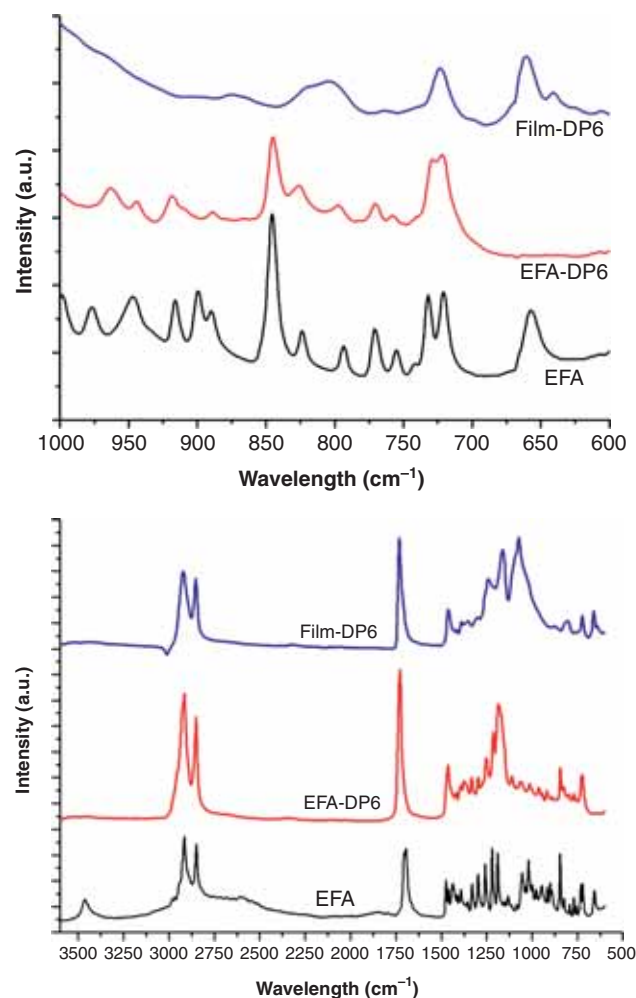


Figure 6 FT-IR spectra of EFA-DP6 before cure and film-DP6 after cure of the oligoester, with (a) a broader range of measure, and (b) focus on a narrow range with the oxirane ring vibration appearing at 845 cm^{-1} .

successful crosslinking to very high conversion due to the complete disappearance of the ring vibration signal of the epoxy group at 845 cm^{-1} (Figure 6b). Corresponding spectra were also obtained for DP3 and DP9 (see supplementary information). It is also observed that the hydroxyl stretching band from $3500\text{--}3700\text{ cm}^{-1}$ is present for EFA, but is no longer observed in the oligomer or film, confirming successful endcapping with hexyl octanoate (Figure 6b).

This further illustrates that the epoxy groups remain available for further epoxy homopolymerization. In addition, the oxirane conversion does not appear to decrease with increasing chain length, or higher oligoester DPs, as the reaction proceeds and the chains become less mobile and locked into place as was expected.

4.1.5 Thermal Properties

The thermal properties of the monomer, synthesized polyesters and crosslinked films were determined by DSC and TGA measurements. Figure 7 shows a DSC diagram comparing the thermal character of EFA, DP9-EFA, and the resulting thermoset film. The thermal characteristics obtained by DSC are also reported in Table 5.

The DSC diagrams for DP 3 and DP 6 are shown in the appendix. The performed DSC measurements show that the monomer has the highest melting point and the highest degree of crystallization compared to the obtained products. The polyesters obtained by enzyme-catalyzed polymerizations show two melting points. The origin of the presence of these two melting points could be due to two different crystal forms that have been observed in previous CalB catalyzed polymers [17, 18], and is a point for future investigation. As noted in Figure 7, the monomer

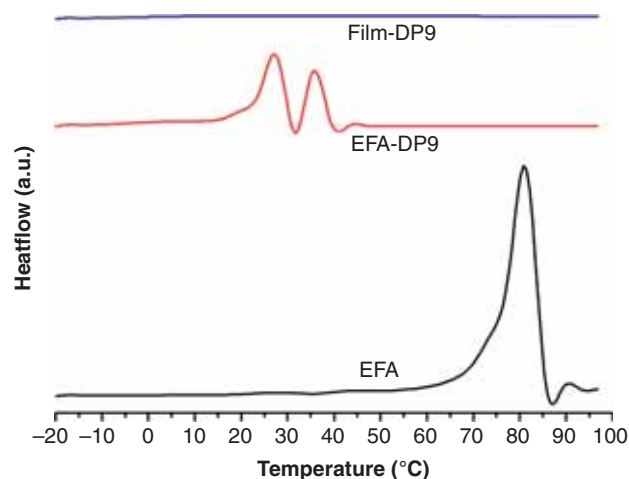


Figure 7 DSC curves of EFA, EFA-DP9, and film-DP9.

Table 5 Thermal properties of the monomer and oligomers.

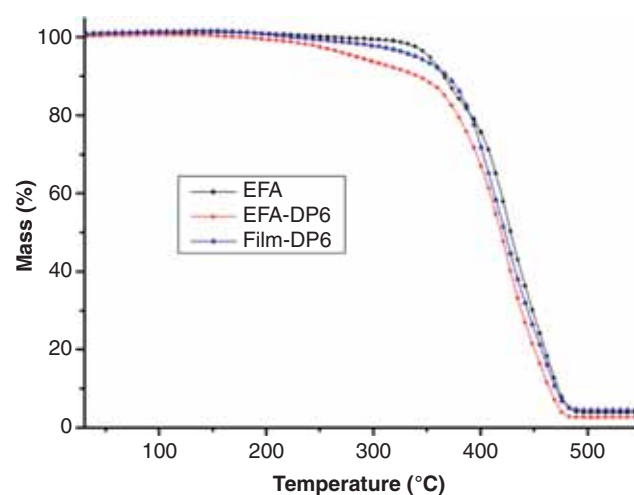
Resin	T_d (°C)	T_g (°C)	T_m (°C)	ΔH_m (J g ⁻¹)
EFA	346	/ ^a	82	151
EFA-DP3	390	/ ^a	31	25
film-DP3	371	-19 ^c	/ ^a	/ ^a
EFA-DP6	385	/ ^a	27 (35) ^b	42 (24) ^b
film-DP6	379	-13 ^c	/ ^a	/ ^a
EFA-DP9	390	/ ^a	28 (36) ^b	42 (21) ^b
film-DP9	383	6 ^c	/ ^a	/ ^a

^a non- detectable.^b second melting point in brackets.^c Tg midpoint with a final temperature ramp of 20°C/min.

EFA has a high degree of crystallization and a melt temperature of approximately 80°C, while after oligomerization it has a large reduction in the melt temperature to approximately 30°C and a decrease in the degree of crystallization (about 70–85% reduction according to the enthalpy of melt values found in Table 5). This lower degree of crystallinity and melting point are likely an effect of the addition of the aliphatic end-capping chains where there were previously carbonyl and hydroxyl groups. These aliphatic chain ends could create more free volume, and the reduction in hydroxyl and carbonyl groups would reduce H-bonding. This effect was also observed by Luciani *et al.* when dendrimer hydroxyl end groups were replaced with aliphatic chains causing a marked decrease in the thermal transitions [25]. Furthermore, no melting points could be observed for the cross-linked polyesters indicating amorphous films, due to the restricted chains between crosslinks that most likely do not have enough mobility to form crystalline lamella. It was difficult to detect a T_g of the films at a temperature ramp of 10°C/min, however at a faster temperature rate (20°C/min) the T_g transition became visible. It is observed that the T_g increases from -26 to -8°C as the DP increases, due to the higher degree of crosslinking relative to chain ends. Further, it was not possible to detect the T_g by DSC of the polyester oligomers, most likely due to their high crystallinity, and thus low degree of amorphous content, providing a weaker signal.

Figure 8 shows the TGA diagram for DP6 monomer, oligoester, and thermoset film.

Additional TGA diagrams corresponding to DP3 and DP9 are presented in the supporting information. The performed TGA measurements reveal the degradation temperatures of the monomer and the obtained products. The monomer has the highest stability until reaching the main degradation

**Figure 8.** TGA diagram of EFA, EFA-DP6, and film-DP6.

temperature of about 350°C. The reason for the differences can be several, but we propose that the end groups present in the oligomers are slightly less stable because the oligomers start to degrade to some extent at lower temperatures. In comparison to this, the thermoset polyesters exhibit less mass decrease due to the presence of a polymeric network based on covalent bonds.

A summary of the thermal properties of the monomer, the polyester oligomers and the crosslinked films is presented in Table 5.

5 CONCLUSIONS

Described in this study is the one-step controlled synthesis of select oligomer lengths with additional end capping using CalB to produce main-chain epoxy

functional oligomers. The oligomers are then further reacted in the absence of side reactions by cationic photopolymerization with the use of an iodium salt photoinitiator to produce thermoset films having a wide range of properties. EFA represents a promising monomer for the design of novel polyesters, which are suitable for further applications due to their versatile epoxy groups.

With respect to the large degree of weight loss after the purification via column chromatography, more efficient eluent mixtures should be investigated to enhance the yield of purified monomers. Furthermore, the synthesized polyester oligomers were not entirely endcapped, which is likely the result of water in the system prohibiting complete reaction. The obtained films after cationically crosslinking the polyester oligomers demonstrated the feasibility of designing amorphous thermoset films with a range of thermal properties depending on the length of the oligoester precursor.

ACKNOWLEDGEMENTS

The Wallenberg Wood Science Center (WWSC), KTH Royal Institute of Technology and the SMP Grant are thanked for their funding. Yvonne Hed is thanked for her help with the Maldi-TOF MS, and Susanne Hansson for help with the size exclusion chromatography. Tommy Iversen at Innventia and Dongfang Li and Monica Ek at the department of Fibre and Polymer Technology, KTH Royal Institute of Technology, are thanked for their important discussion and help with equipment.

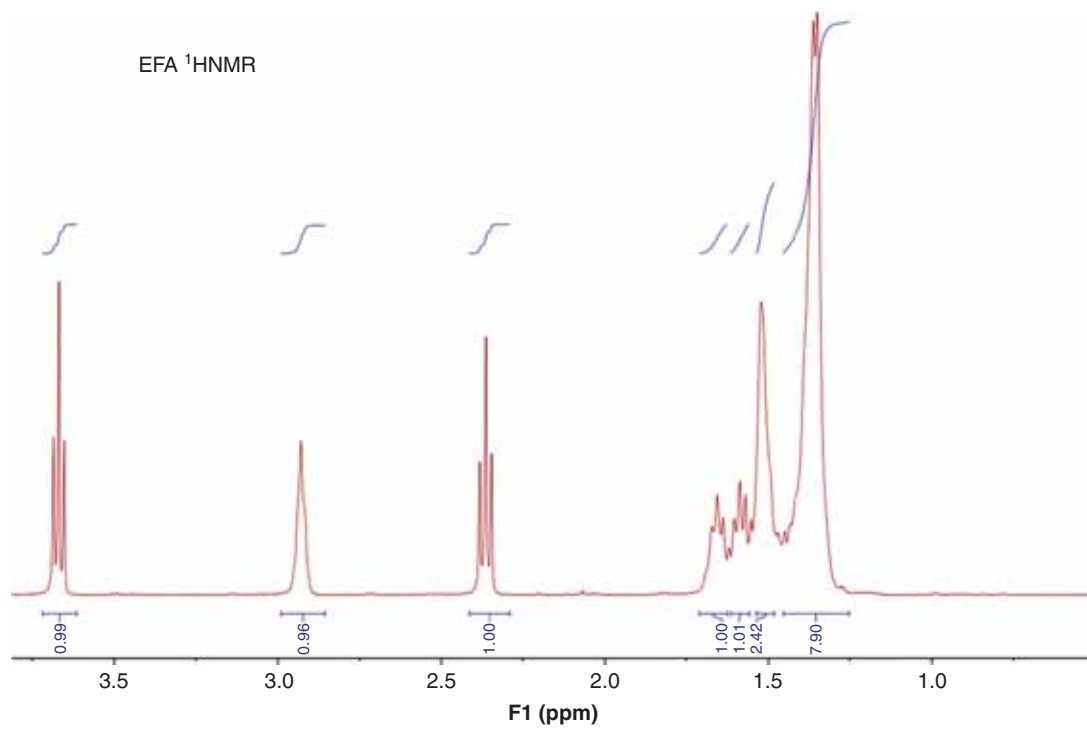
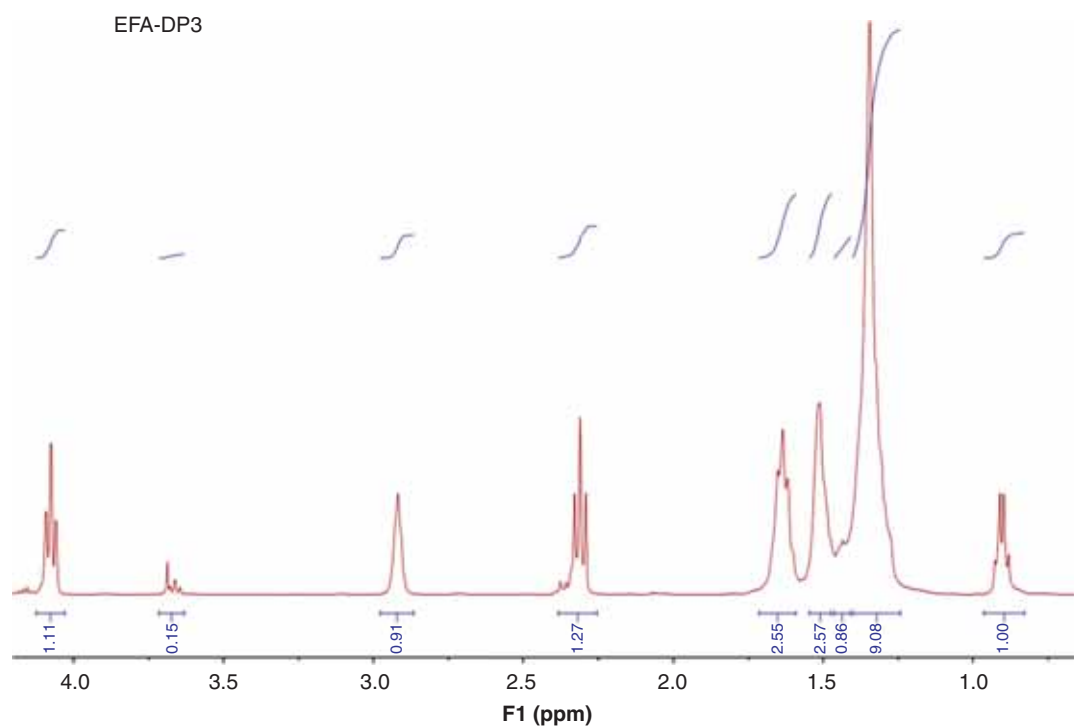
REFERENCES

1. J.E. Holladay, J.F. White, J.J. Bozell, and D. Johnson (Eds), *Top Value-Added Chemicals from Biomass. Volume II: Results of Screening for Potential Candidates from Biorefinery Lignin*. PNNL-16983, Pacific Northwest National Laboratory, U.S. Department of Energy (2007).
2. T. Werpy and G. Peterson (Eds.), *Top Value Added Chemicals from Biomass. Volume I: Results of Screening for Potential Candidates from Sugars and Synthesis Gas*. U.S. Department of Energy, (2004).
3. F.S. Guner, Y. Yagci, and A.T. Erciyas, Polymers from triglyceride oils. *Prog. Polym. Sci.* **31**, 633–670 (2006).
4. A. Guo and Z. Petrovic. Industrial Use of Vegetable Oil, in *Vegetable Oils-Based Polyols*, S.Z. Erhan, (Ed.), AOCS Publishing, Champaign, Ill (2005).
5. M.A. Meier, J.O. Metzger, and U.S. Schubert, Plant oil renewable resources as green alternatives in polymer science. *Chem. Soc. Rev.* **36**, 1788–802 (2007).
6. G. Lligadas, J.C. Ronda, M. Galiá, and V.Cádiz, Oleic and undecylenic acids as renewable feedstocks in the synthesis of polyols and polyurethanes. *Polymers* **2**, 440–453 (2010).
7. C. Liu, F. Liu, J. Cai, W. Xie, T.E. Long, S.R. Turner, A. Lyons, and R.A. Gross, Polymers from fatty acids: Poly(ω -hydroxyl tetradecanoic acid) synthesis and physico-mechanical studies. *Biomacromolecules* **12**, 3291–3298 (2011).
8. J.M. Raquez, M. Deléglise, M.F. Lacrampe, and P. Krawczak, Thermosetting (bio)materials derived from renewable resources: A critical review. *Prog. Polym. Sci.* **35**, 487–509 (2010).
9. M.K.G. Johansson, M. Svensson, P.E. Sundell, Method for production of thermally cured coatings, US Patent 7,799,386 B2, (September 21, 2010).
10. M. Claudino, I. van der Meulen, S. Trey, M. Jonsson, A. Heise, and M. Johansson, Photoinduced thiol-ene cross-linking of globalide/ ϵ -caprolactone copolymers - curing performance and resulting thermoset properties. *J. Polym. Sci. A1* **50**, 16–24 (2012).
11. Y. Xia and R.C. Larock, Vegetable oil-based polymeric materials: synthesis, properties, and applications. *Green Chem.* **12**, 1893–1909 (2010).
12. L. Montero de Espinosa and M.A.R. Meier, Plant oils: The perfect renewable resource for polymer science?! *Eur. Polym. J.* **47**, 837–852 (2011).
13. M.F. Demirbas, Biorefineries for biofuel upgrading: A critical review. *Appl. Energ.* **86**, S151–S161 (2009).
14. R. Ekman, The suberin monomers and triterpenoids from the outer bark of *Betula verrucosa* Ehrh. *Holzforchung* **37**, 205–211 (1983).
15. P. Pinto, A.F. Sousa, A. Silvestre, C.P. Neto, A. Gandini, C. Eckerman, and B. Holmbom, *Quercus suber* and *Betula pendula* outer barks as renewable sources of oleochemicals: A comparative study. *Ind. Crop. Prod.* **29**, 126–132 (2009).
16. P.A. Krasutsky, Birch bark research and development. *Nat. Prod. Rep.* **23**, 919–942 (2006).
17. P.A. Kratusky, R.M. Carlson, V.V. Nesterenko, I.V. Kolomitsyn, and C.F. Edwardson, Birch bark processing and isolation of natural products from birch bark, US Patent 6,392,070 B1, (2002).
18. A. Gandini, C.P. Neto, and A.J.D. Silvestre, Suberin: A promising renewable resource for novel macromolecular materials. *Prog. Polym. Sci.* **31**, 878–892 (2006).
19. A. Olsson, M. Lindström, and T. Iversen, Lipase-catalyzed synthesis of an epoxy-functionalized polyester from the suberin monomer *cis*-9,10-epoxy-18-hydroxyoctadecanoic acid. *Biomacromolecules* **8**, 757–760, (2007).
20. J.P. Douliez, J. Barrault, F. Jerome, A. Heredia, L. Navailles, and F. Nallet, Glycerol derivatives of cutin and suberin monomers: Synthesis and self-assembly. *Biomacromolecules* **6**, 30–34 (2005).
21. J.A. Heredia-Guerrero, A. Heredia, R. García-Segura, and J.J. Benítez, Synthesis and characterization of a plant cutin mimetic polymer. *Polymer* **50**, 5633–5637 (2009).
22. A.F. Sousa, A.J.D. Silvestre, A. Gandini, C.P. Neto, Synthesis of aliphatic suberin-like polyesters by eco-friendly catalytic systems. *High Performance Polymers* **24**, 4–8 (2012).
23. A.F. Sousa, A. Gandini, A.J.D. Silvestre, C.P. Neto, J.J.C. Pinto, C. Eckerman, and B. Holmbom, Novel suberin-based biopolyesters: From synthesis to properties. *J. Polymer Sci. Part A* **49**, 2281–2291 (2011).

24. A.F. Sousa, A. Gandini, A.J. Silvestre, and C.P. Neto, Synthesis and characterization of novel biopolyesters from suberin and model comonomers. *ChemSusChem*. **1**, 1020–1025 (2008).
25. M. Eriksson, K. Hult, E. Malmström, M. Johansson, S. Trey, and M. Martinelle, One-pot enzymatic polycondensation to telechelic methacrylate-functional oligoesters used for film formation. *Polym. Chem.* **2**, 714–719 (2011).
26. M. Eriksson, L. Fogelström, K. Hult, E. Malmström, M. Johansson, S. Trey, and M. Martinelle, Enzymatic one-pot route to telechelic poly(pentadecalactone) epoxide: Synthesis, UV curing, and characterization. *Biomacromolecules* **10**, 3108–3113 (2009).
27. R.A. Gross, M. Ganesh, and W. Lu, Enzyme-catalysis breathes new life into polyester condensation polymerizations. *Trends Biotechnol.* **28**, 435–443 (2010).
28. R.T. Mathers and M.A.R. Meier, (Eds.), *Green Polymerization Methods: Renewable Starting Materials, Catalysis and Waste Reduction*, Wiley-VCH Verlag GmbH & Co. KGaA, Weinheim, Germany (2011).
29. Y. Yu, D. Wu, C. Liu, Z. Zhao, Y. Yang, and Q. Li, Lipase/esterase-catalyzed synthesis of aliphatic polyesters via polycondensation: A review. *Process Biochem.* **47**, 1027–1036 (2012).
30. K. Hult and P. Berglund, Enzyme promiscuity: Mechanism and applications. *Trends Biotechnol.* **25**, 231–238 (2007).
31. S. Dai, L. Xue, M. Zinn, and Z. Li, Enzyme-catalyzed polycondensation of polyester macrodiols with divinyl adipate: A green method for the preparation of thermoplastic block copolyesters. *Biomacromolecules* **10**, 3176–3181 (2009).
32. P. Lozano, T. de Diego, D. Carrié, M. Valutier, and J.L. Iborra, Lipase catalysis in ionic liquids and supercritical carbon dioxide at 150°C. *Biotechnol. Prog.* **19**, 380–382 (2003).
33. B. Golaz, V. Mouchaud, Y. Leterrier, and J.-A.E. Månson, UV intensity, temperature and dark-curing effects in cationic photo-polymerization of a cycloaliphatic epoxy resin. *Polymer* **53**, 2038–2048 (2012).
34. M. Sangermano, M. Messori, M. Martin Galleco, G. Rizza, and B. Voit, Scratch resistant tough nanocomposite epoxy coatings based on hyperbranched polyesters. *Polymer* **50**, 5647–5652 (2009).
35. E.W. Nelson, J.L. Jacobs, A.B. Scranton, K.S. Anseth, and C.N. Bowman, Photo-differential scanning calorimetry studies of cationic polymerizations of divinyl ethers. *Polymer* **36**, 4651–4656 (1995).
36. J.V. Crivello, Cationic polymerization — Iodonium and sulfonium salt photoinitiators, in *Initiators — Poly-Reactions — Optical Activity* (Advances in Polymer Science, Vol. 62), pp. 1–48, Springer, Berlin (1984).
37. M.A. Tehfe, J. Lalevée, X. Allonas, and J.P. Fouassier, Long wavelength cationic photopolymerization in aerated media: A remarkable titanocene/tris(trimethylsilyl)silane/onium salt photoinitiating system. *Macromolecules* **42**, 8669–8674 (2009).
38. P.E. Sundell, S. Jönsson, and A. Hult, Photo-redox induced cationic polymerization of divinyl ethers. *J. Polym. Sci. A1: Polym. Chem.* **29**, 1525–1533 (1991).
39. J.R. Kim and S. Sharma, The development and comparison of bio-thermoset plastics from epoxidized plant oils. *Ind. Crop. Prod.* **36**, 485–499 (2012).
40. A.E. Gerbase, C.L. Petzhold, and A.P.O. Costa, Dynamic mechanical and thermal behavior of epoxy resins based on soybean oil. *J. Am. Oil Chem. Soc.* **79**, 797–802 (2002).
41. STFI-Packforsk AB, New method for isolation of suberin products from birch bark. W.I.P. Organization (2010).
42. A. Luciani, C.J.G. Plummer, T. Nguyen, L. Garamszegi, J.-A.E. Månson, Rheological and physical properties of aliphatic hyperbranched polyesters. *J. Polym. Sci. B: Polym. Phys.* **42**, 1218–1225 (2004).

SUPPLEMENTARY INFORMATION

1 NMR Spectra:

Figure 1 $^1\text{H NMR}$ spectrum of EFA.Figure 2 $^1\text{H NMR}$ spectrum of EFA-DP3

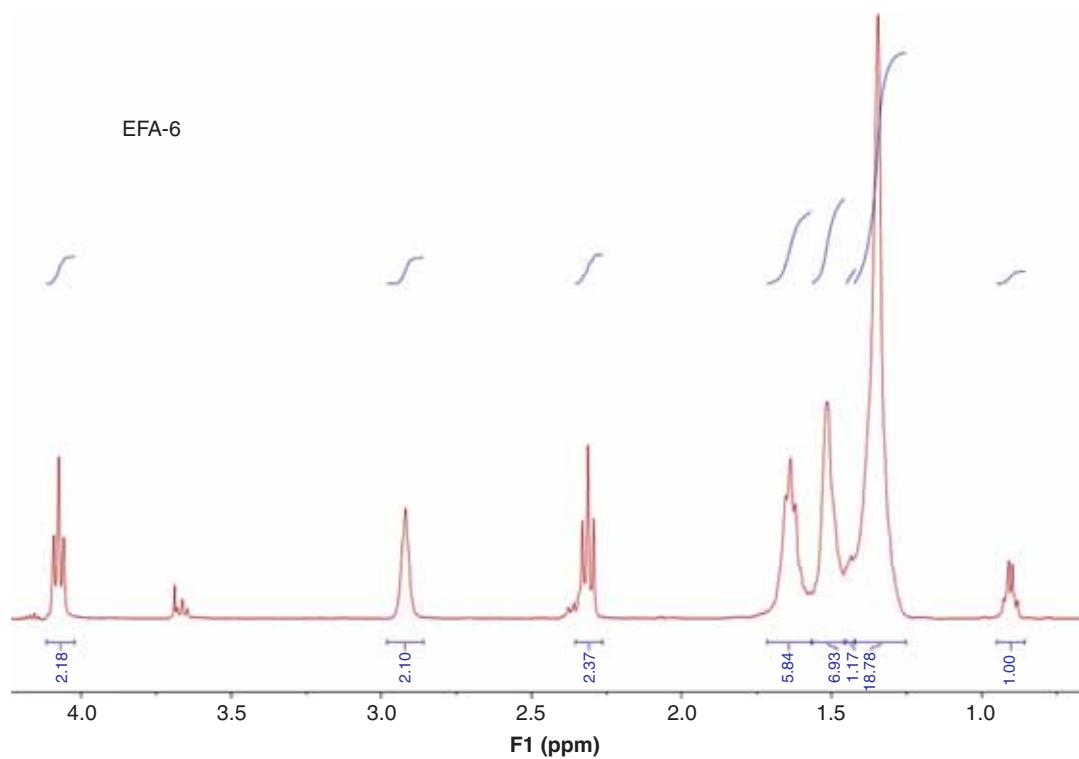


Figure 3 ¹H NMR spectrum of EFA-DP6

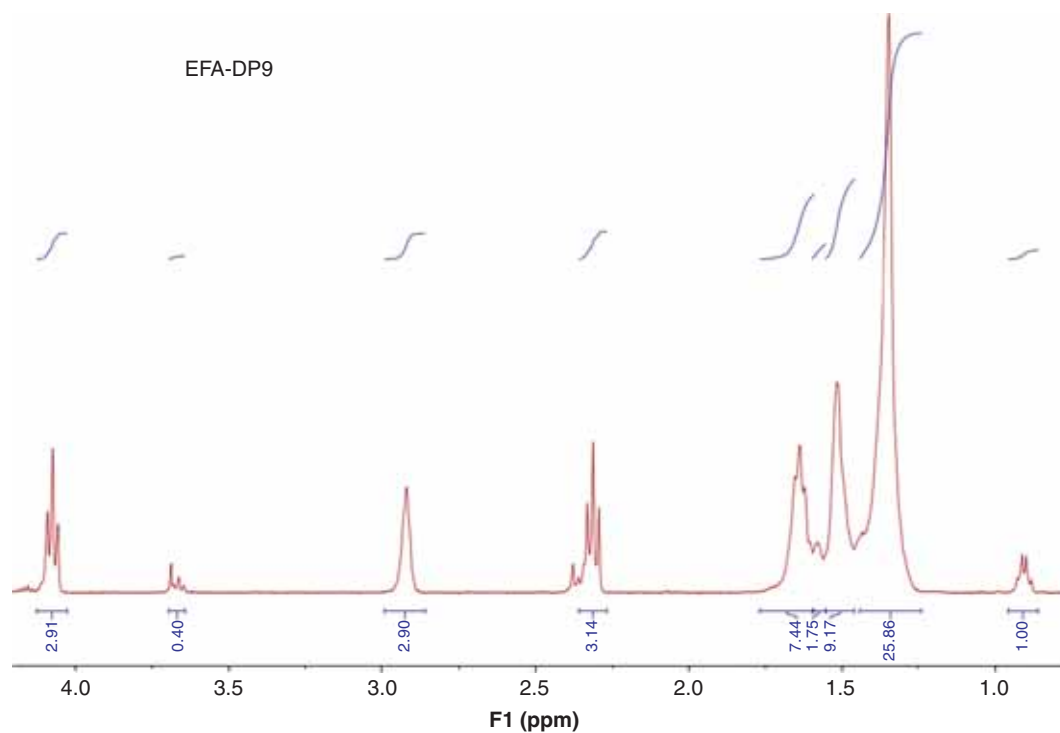


Figure 4 ¹H NMR spectrum of EFA-DP9

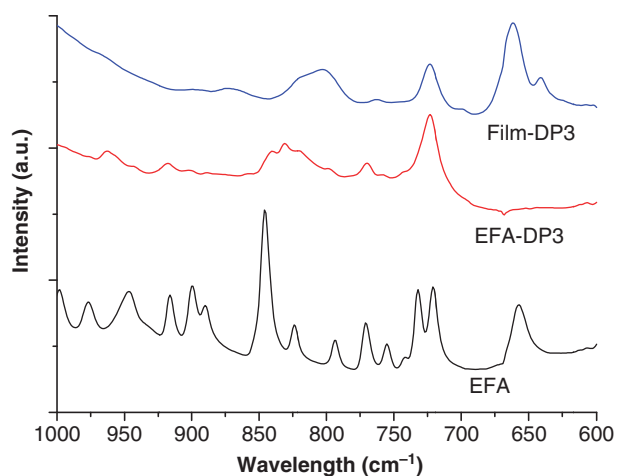


Figure 5 FT-IR spectrum of EFA, EFA-DP3, and the thermoset film-DP3.

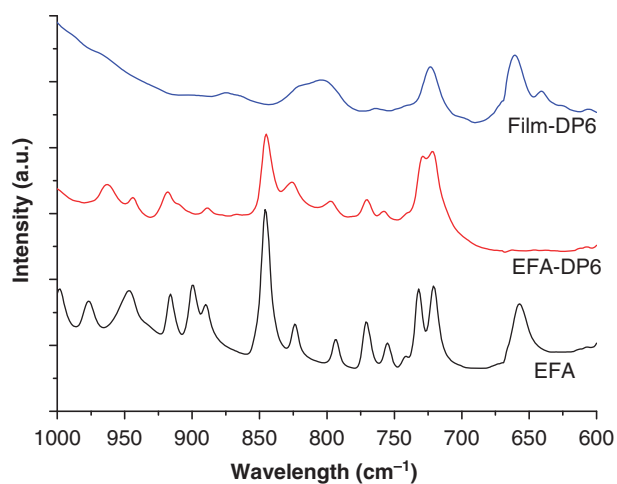


Figure 6 FT-IR spectrum of EFA, EFA-DP6, and the thermoset film-DP6.

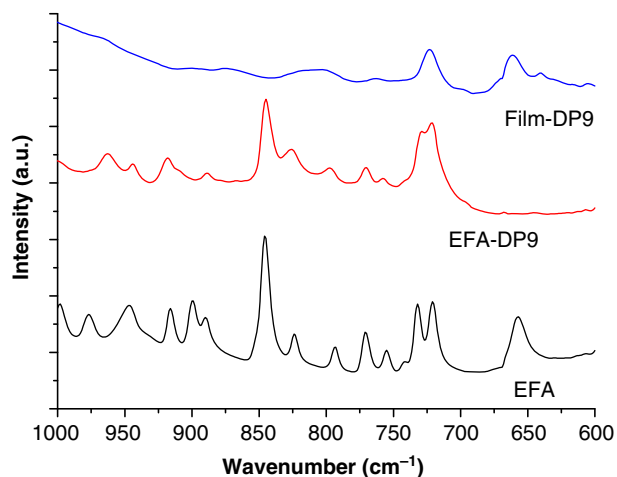


Figure 7 FT-IR spectrum of EFA, EFA-DP9, and the thermoset film-DP9.

Dynamic Scanning Calorimetry plots:

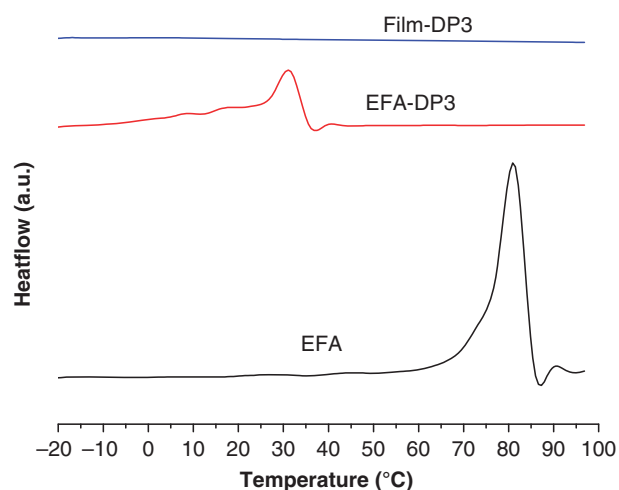


Figure 8 DSC plot of EFA, EFA-DP3, and the thermoset film-DP3.

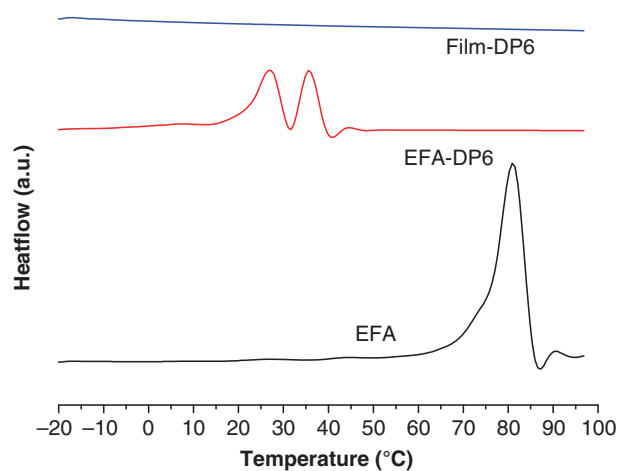


Figure 9 DSC plot of EFA, EFA-DP6, and the thermoset film-DP6.

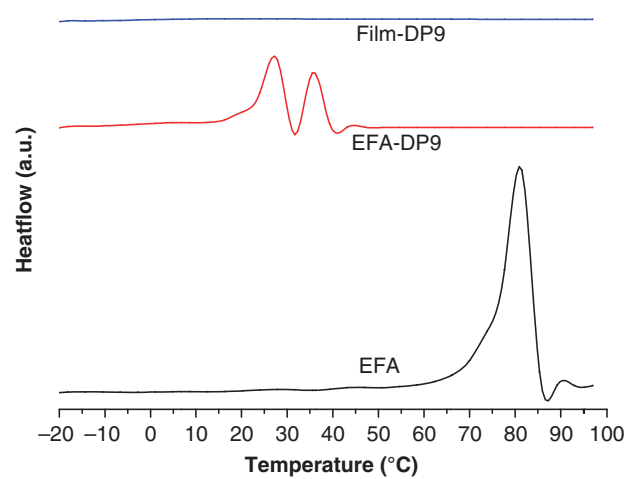


Figure 10 DSC spectrum of EFA, EFA-DP9, and the thermoset film-DP9.

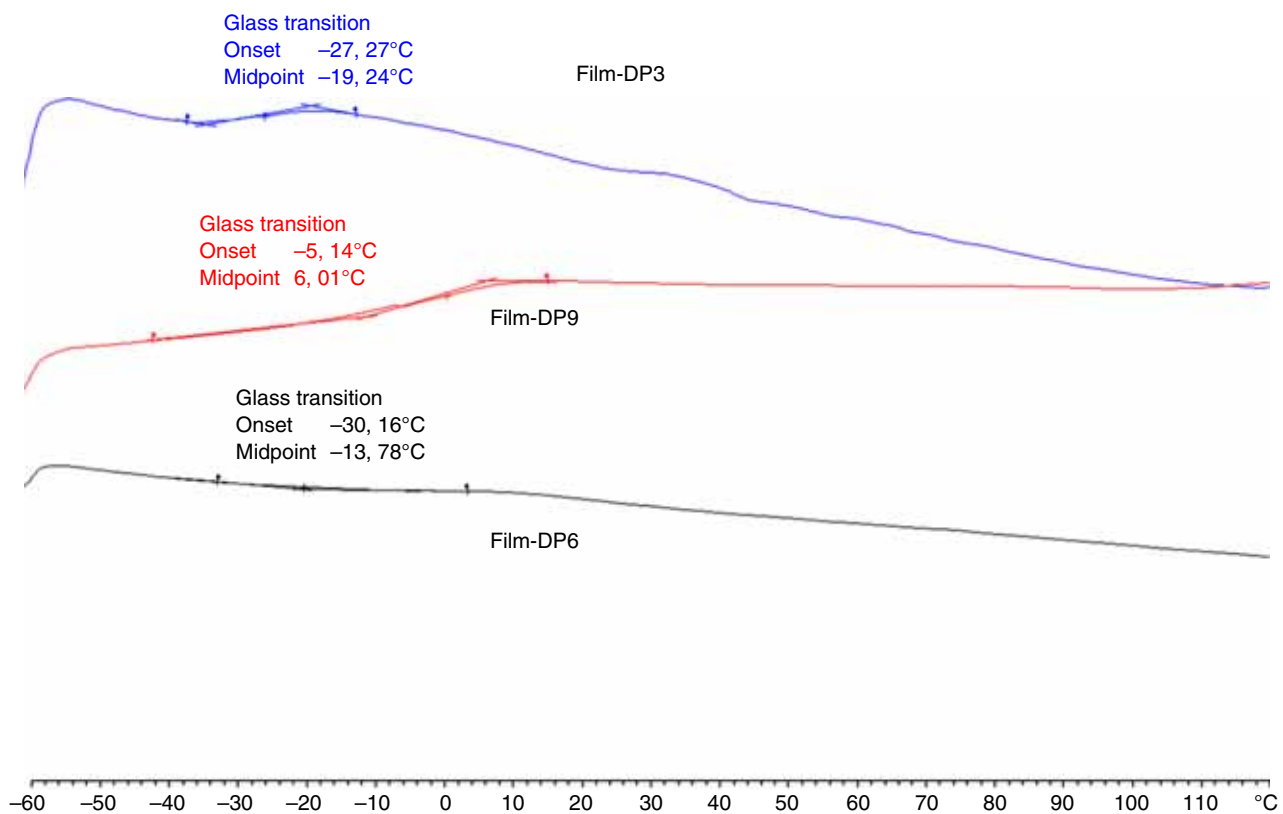


Figure 11 DSC plots of film-DP3, film-DP6, and film-DP9.

Thermogravimetric Analysis Plots:

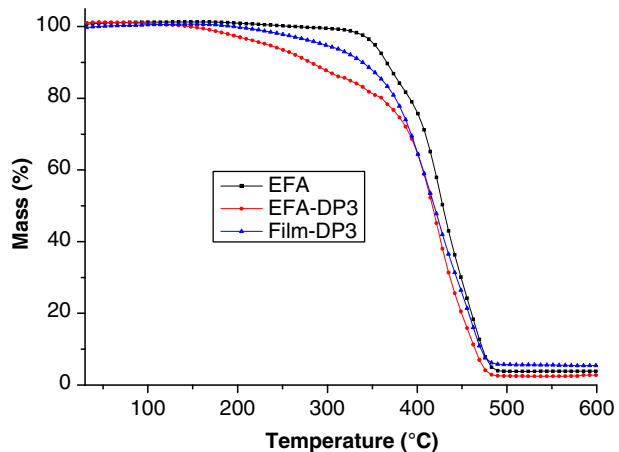


Figure 12 TGA plot of EFA, EFA-DP3, and the thermoset film-DP3.

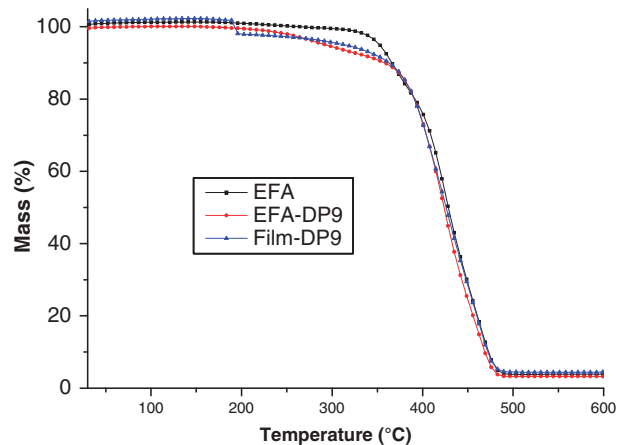


Figure 14 TGA plot of EFA, EFA-DP9, and the thermoset film-DP9.

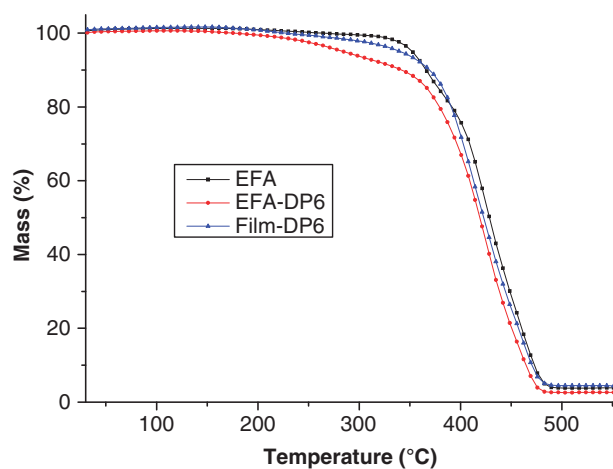


Figure 13 TGA plot of EFA, EFA-DP6, and the thermoset film-DP6.